



Contributions of urban green and blue spaces on local-scale climate in the core area of Beijing, China

Yilun Li^{1,2} · Shuxin Fan^{1,3,4} · Kun Li⁵ · Kaien Ke⁶ · Li Dong^{1,3,4}

Accepted: 8 July 2023 / Published online: 29 July 2023

© The Author(s), under exclusive licence to Springer Science+Business Media, LLC, part of Springer Nature 2023

Abstract

Construction of urban green and blue spaces (UGBS) has long been proved as an effective mitigation to urban heat island effect. Yet we spotted a rarity of studies evaluating UGBS's climatic effect difference in different land-uses, and a rarity of empirical evidence on better UGBS allocation for better cooling. In this study, we conducted field measurements of nighttime air temperature (Ta) and relative humidity (Rh) along an enclosed transect at the core area of Beijing, China, and evaluated the contributions of UGBS on local-scale climate. Land-cover types and land-use classification scheme Local Climate Zone (LCZ) were used to analyze measured Ta and Rh. Urban vegetation coverage is further intersected with LCZs to evaluate vegetation's cooling and humidifying effects in different land-uses. Results show that better correlations were generally detected with larger buffer zones when more land-cover and land-use conditions were included. UGBS exhibit significant cooling and humidifying effects, and better regression models were built when green and blue spaces were taken as a whole rather than independently. Coverage of LCZ 1 (compact high-rise), LCZ 2 (compact midrise) and LCZ G (water coverage) were found to more significantly contribute to local-scale climate. Increasing vegetation coverage in LCZ 2 and LCZ 3 is expected to facilitate better cooling and humidifying effect. Results of this study may provide insights for practitioners to allocate UGBS for better urban cooling.

Keywords Urban vegetation · Urban green space · Local Climate Zone (LCZ) · Air temperature · Relative humidity · Land use/land cover (LULC)

Introduction

Induced and exacerbated by human activity and urban expansion, the urban heat island (UHI) effect, a phenomenon featuring higher temperatures in urban areas than in

surrounding rural areas (Oke 1982), is a serious urban threat awaiting solutions. While the construction of urban green and blue spaces (UGBS) has long been proved as an effective mitigation (Bowler et al. 2010; Demuzere et al. 2014; Gago et al. 2013; Gunawardena et al. 2017). Aiming at providing references to planning and design practice, composition (e.g., Yu et al. 2020) and configuration (e.g., Guo et al.

Yilun Li and Shuxin Fan contributed equally to this paper.

✉ Li Dong
dongli@bjfu.edu.cn

Yilun Li
yilun595@connect.hku.hk

Shuxin Fan
fanshuxin_09@bjfu.edu.cn

Kun Li
kunli@zafu.edu.cn

Kaien Ke
kanekelion@163.com

² Division of Landscape Architecture, Faculty of Architecture, The University of Hong Kong, Hong Kong SAR, China

³ Laboratory of Urban and Rural Ecological Environment, Beijing 100083, China

⁴ National Engineering Research Center for Floriculture, Beijing 100083, China

⁵ College of Landscape Architecture and Architecture, Zhejiang A&F University, Hangzhou 311300, China

⁶ School of Forestry, Beijing Forestry University, Beijing 100083, China

¹ School of Landscape Architecture, Beijing Forestry University, 35, Qinghua East Rd., 100083 Beijing, China

2020; Wang et al. 2022; Zhou et al. 2011) of UGBS have been vastly evaluated from the perspective of land-cover and land-use, which are recognized as key drivers to urban climate heterogeneity (Dan et al. 2022) and key considerations in planning and design practice (Eliasson 2000).

Targeted at planning issues, past analyses on urban thermal environment from land-use perspective have adopted multiple classification schemes. Adoption of local policy-based land-use classification (e.g., Masoudi et al. 2021; Weber et al. 2014) and urban functional zones (e.g., Ke et al. 2021; Li et al. 2021a, b) well echoes domestic planning policy and land functions. Higher temperatures were generally observed in commercial and residential areas (Dorigon and Amorim 2019; Sun et al. 2013, 2018), while ecological lands with higher vegetation and water coverage are usually cold and wet islands (Chen et al. 2019; Shi et al. 2018, 2019; Yang et al. 2020). However, policy and function-based classification schemes lack considerations of links between urban form and corresponding thermal property, which is addressed by multiple evolving climatic based land-use classification schemes, e.g., Urban Terrain Zone (UTZ) (Ellefsen 1991), Urban Climate Zone (UCZ) (Oke 2005), and Local Climate Zone (LCZ) (Stewart and Oke 2012). Among these classification schemes, LCZ scheme has been widely applied in urban climate studies (Aslam and Rana 2022), resulting from three major improvements compared to other climatic based land-use classification schemes, i.e., usage of a full set of surface climate properties, inclusion of rural landscapes, universal class names and definitions across urban settings (Stewart and Oke 2012).

While analysis evaluating the difference of UGBS's climatic effects in different land-uses remains rare, which may give direct references to practitioners on where to allocate UGBS for more effective cooling. Such analysis requires intersections of land-use and land-cover perspectives. Previous related studies have evaluated the climatic effects of UGBS in different local policy-based land-use classification types (Masoudi et al. 2021) and urban functional zones (Connors et al. 2012; Ke et al. 2021; Li et al. 2021a, b), while climatic-based land-use classification schemes have been less utilized. Though by using LCZ classification, linkage between vegetation coverage and different LCZs have been built and used for planning scenario evaluation (Alexander et al. 2016), detailed empirical evidence of UGBS's climatic effect in different LCZs is still needed.

Additionally, most studies on UGBS's climatic effects have utilized land surface temperature as temperature indicator (e.g., Masoudi et al. (2021); Connors et al. (2012)), largely due to its easy access to cover a wide geospatial range. Though it is regarded as a valid proxy to understand Ta variance (Amani-Beni et al. 2022), empirical study on the response of field measured Ta to UGBS remains rare and is still needed considering their different diurnal and seasonal

pattern (Grimmond 2007; Hu et al. 2019), diverging intensity (Derdouri et al. 2021), and closer linkage between Ta and human thermal comfort (Nie et al. 2022).

In light of these, we conducted field measurements of Ta and Rh along a traverse at core Beijing, China, and evaluated UGBS's local-scale climatic effect in different land-use represented by LCZ. The objectives of this study are (1) to evaluate how and to what spatial scale does Ta and Rh responds to UGBS and different land-use represented by LCZ, and (2) to examine if climatic effects of UGBS differ among different LCZs in densely built urban area. Results of this study is expected to provide empirical evidence for practitioners on better allocation of UGBS for better local-scale cooling.

Methodology

Study sites

Beijing (39°56'N, 116°20'E), the capital city of China, locates in the northwest of North China Plain and has a total area of 16410 km². It has a warm temperate semi humid continental monsoon influenced climate. In 2019, the annual precipitation was 406.3 mm; the annual average air temperature was 13.8 °C; and the average air temperatures of July and August were 28.0 °C and 25.9 °C respectively (NBSC 2020). It suffers severe UHI issues as the city expands over past several decades (Peng et al. 2016).

The 2nd Ring Rd. of Beijing, built in 1992 and with a total length of 32.7km, is an enclosed circular expressway located at the core area of Beijing, as shown in Fig 1. Multiple large urban green spaces, e.g., Tiantan Park (The Temple of Heaven), Longtanhu Park, Taoranting Park, etc., are located along the 2nd Ring Rd. Though water coverage is generally rare, a linear-shaped park with a canal running through and several manmade lakes mostly with impervious water edges are around. In addition, diversified land-use exist along the road, making it a good sampling route to analyze how UGBS, as well as their interaction with land-use, contribute to local scale climate. Frequent urban renovation and construction of new green and blue spaces aim at providing ecological benefits to the city and are in demand of further knowledge on constructing a sustainable city.

Measurement of air temperature and relative humidity

Mobile measurements of Ta and Rh were conducted by using a HOBO MX2302A External Temperature / Rh Sensor Data Logger mounted to a car at the height of approximately 2m at 1s interval. The accuracy of the device is ± 0.2 °C and $\pm 2.5\%$, and the resolution is 0.1 °C and 0.1%, meeting the requirements of ISO 7726 (International Standard Organization

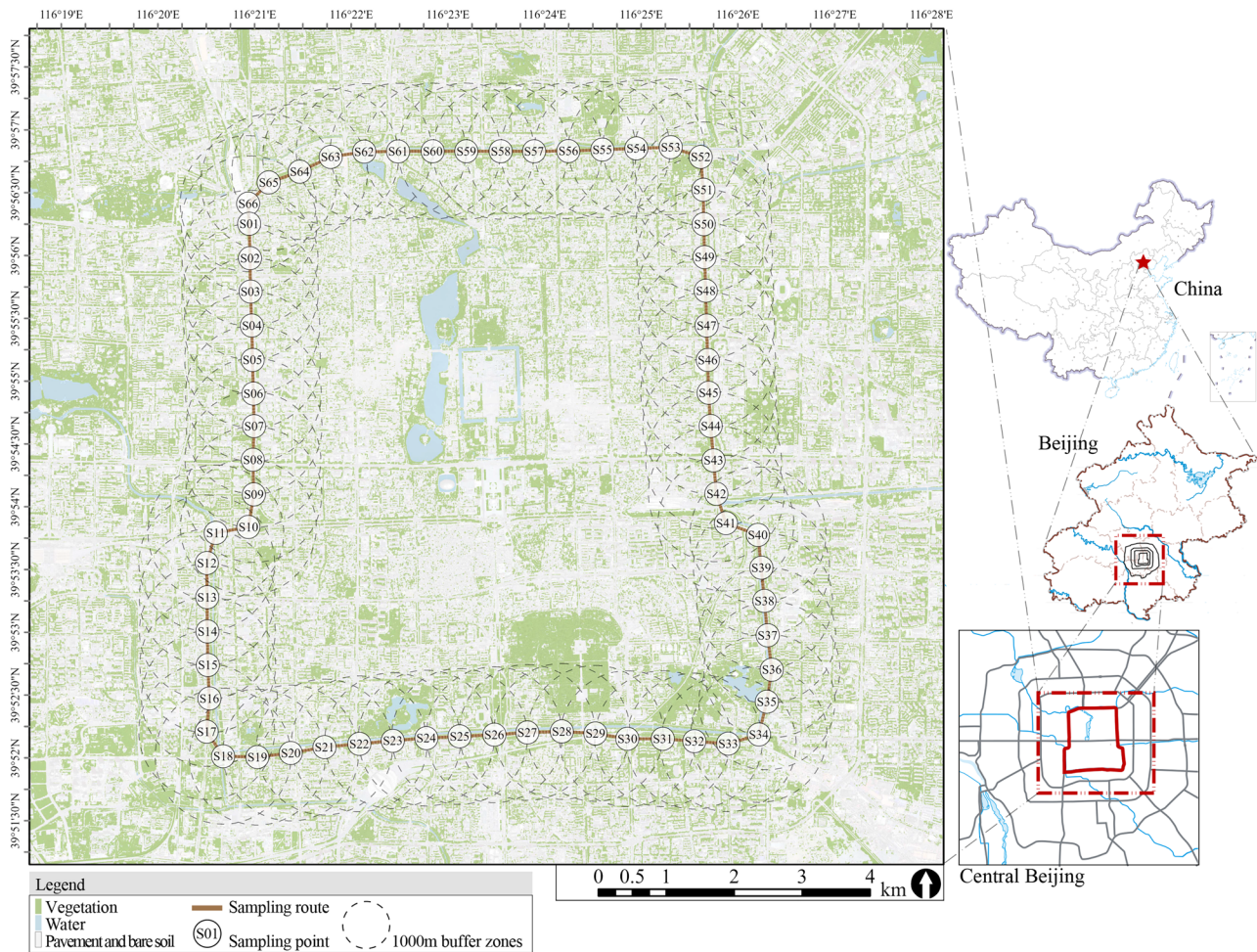


Fig. 1 Study site and locations of sampling points with land-cover classification results in summer

1998). The device was fixed in a cuboid carton with two open ends (30cm×10cm×12cm) wrapped by insulation materials horizontally fixed on the top of a car. Considering that urban heat island effect peaks several hours after sunset in temperate regions (Doick et al. 2014; Oke et al. 2017), data samplings were conducted at night in summer (23:00–24:00, Aug. 17 and 18, 2019) and winter (22:30–23:30, Jan. 29 and 30, 2020). It is also during this time that very few cars travel on street, thus enabling a drive at a stable speed and minimizing the influence from the anthropogenic heat from other vehicles. Due to the minimum car speed limit on the 2nd Ring Rd, the car was driven at a speed of approximately 60 km/h, resulting in each data sampling process less than 30 min. Such driving speed approximates the maximum driving speed in previous research that have used similar data sampling method (Leconte et al. 2015; Shi et al. 2018). A total of 66 sampling points each with 500m away from its adjacent ones, which is considered a typical horizontal scale of city block unit (Oke 2005), were selected, as shown in Fig 1. UniStrong UG908 GPS Terminal was used to record the geographical location

and time, based on which Ta and Rh data were matched afterwards. Background meteorology conditions during sampling time were listed in Appendix A.

Measurement of influencing factors

Measurement of land-cover and land-use composition

To investigate how UGBS influence local-scale climate, land-cover classification around data sampling routes were performed by using GF-2 image with four multi-spectral bands (4m resolution) and 1 panchromatic band (0.8m resolution). Image acquired on Aug. 31, 2018 (L1A0003421879) and Sep. 5, 2018 (L1A0003433834) were used for land-cover classification in summer, while data acquired on Dec. 13, 2017 (L1A0002844943、L1A0002844938) were used for winter. Atmospheric and geometric correction were conducted by using ERDAS. We then combined supervised classification and visual interpretation to identify three land-cover types, namely vegetation, water body and impervious surfaces. In this study,

UGBS are composed of urban green spaces and urban blue spaces, with the former referring to areas that feature vegetation coverage (Taylor & Hochuli 2017), and the latter referring to all forms of natural and manmade surface water (Smith et al. 2021). We didn't further specify different vegetation types, as we focus more on UGBS's allocation, i.e., a planning perspective, instead of the configuration of different vegetation types, which is more of a design issue. Taking urban vegetation as a whole can well address this purpose.

Supervised classification of vegetation and non-vegetation was conducted in QGIS 3.22.2 with dzetsaka by using Gaussian Mixture Model (Karasiak 2016), while water bodies were visually interpreted. Land-cover maps of the three land-cover types were further produced by subtracting visually interpreted water body area from non-vegetation area. The overall Kappa coefficient of the land-cover classification were 0.82 and 0.80 for summer and winter respectively, evaluated by using 216 randomly generated points. Land-cover classification results in summer are shown in Fig. 1.

To investigate how land-use contribute to local scale climate, we classified the land around the sampling routes following the LCZ scheme. Though raster-based LCZ maps covering wide spatial range have been successfully generated by data fusion (Zhou et al. 2021), considering that this research is of fine scale, we still performed visual interpretation for LCZ classification to generate LCZ maps around the sampling route, which is less effective and repeatable in

future studies. GF-2 image and Baidu maps were used for visual identification of street networks and building density and height. Field investigation on building height was conducted when necessary to distinguish between LCZ types.

To investigate if the relationships between Ta, Rh and land-cover, land-use factors are scale-dependent, buffer zones were generated around each sampling points with radii of 100m, 200m, 300, 400m, 500m, 600m, 700m, 800m, 900m and 1000m. The largest buffer zone radius is restricted to 1000m, for it is regarded as the typical horizontal scale of local-scale climate (Oke et al. 2017), and local green spaces' climatic effect on Ta and Rh at night extend as far as around 1km (Li et al. 2021a, b; Yan et al. 2018). The coverage ratios of each land-cover type, as well as each LCZ, were calculated for buffer zones of different radius. The land-cover and LCZ composition within 1000m buffer zones around each sampling points are shown in Fig. 2.

Measurement of UGBS in different land-uses

To further investigate if the climatic effects of UGBS in different LCZ types vary, we further intersected the generated land-cover maps and LCZ maps to calculate the vegetation coverage in LCZ 1-6. Water coverage was not considered in this part of analysis as its rarity in the analyzed buffer zones (Fig. 2a). These LCZ types were selected, for they are main components around the sampled area. All geographical data were processed in QGIS 3.22.2.

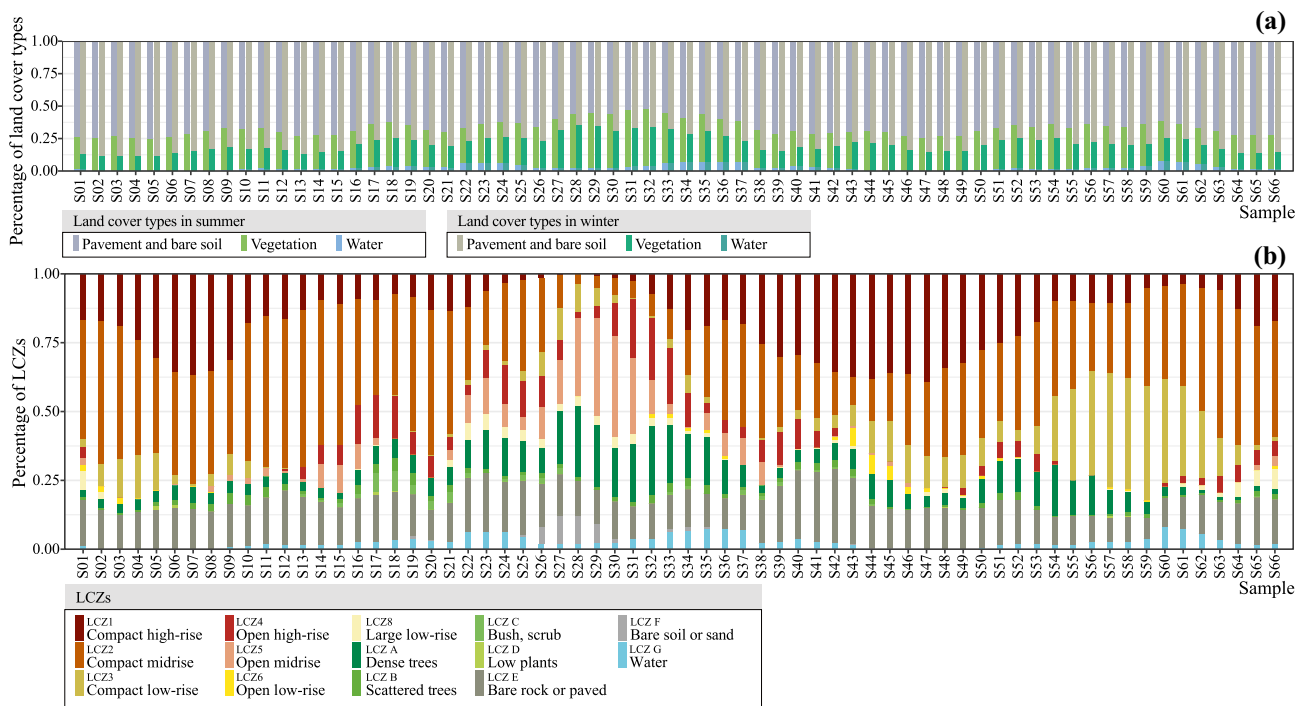


Fig. 2 Coverage of **a** different land-cover types in summer and winter and **b** different LCZs within 1000m buffer zones around each sampling point

Data analyses

Ta and Rh at each sampling point were extracted from the logged data by matching with the GPS records. To avoid accidental data variations, we calculated a 7s-average Ta and Rh to represent data at each sampling point, which contains 3s before and 3s after passing the point. Considering the car speed, such averaged data represents mean Ta and Rh within 100m distance, which falls at the center of the 100m-radius buffer zone, guaranteeing credible buffer zone analysis. However, due to data anomaly caused by routine road maintenance work and bad traffic conditions, Ta and Rh collected at night in summer at samples 34–55 were excluded. Two-day averaged Ta and Rh at each sampling point were calculated for summer and winter respectively for data depiction.

Ta and Rh at each sampling point were centered on a daily basis so that the difference in background meteorology conditions could be eliminated. Pearson correlation coefficients between centered Ta, Rh and the percentage of different land-cover types and LCZs within 100–1000m radius buffer zones were calculated. The buffer zone size with generally the strongest correlation was further used for building regression models.

To quantify and compare the climatic effect of different land-covers and land-use, linear regression models were built with centered Ta and Rh as dependent variables and percentage of different land-cover types and LCZs as independent variables. To compare the significance of different LCZs climatic effects, multiple regression models were built between centered Ta, Rh and the percentage of different LCZs under stepwise algorithm.

Furthermore, to evaluate if the climatic effect of vegetation in different land-use varies, Pearson correlation coefficients and partial correlation coefficients with total vegetation coverage controlled between centered Ta, Rh and vegetation coverage in LCZ 1–6 were calculated.

All data analyses were conducted on R 3.5.3. Graphics were depicted in R and further edited in Adobe Illustrator when needed.

Results

Ta and Rh distribution along sampling route

Descriptive statistics of 2-day averaged Ta and °Rh at all sampling points are given in Table 1. Two-day averaged Ta ranged as high as 1.23 °C and 1.84 °C among all available sampling points at summer and winter night respectively, while two-day averaged Rh ranged 6.95% and 9.61% respectively.

As depicted in Fig. 3 the two-day averaged Ta and Rh profile along sampling routes, certain Ta and Rh trends were shown in the 2-day averaged Ta and Rh profile at

Table 1 Descriptive statistics of two-day averaged Ta and Rh along sampling routes

| | Summer nighttime | Winter nighttime |
|-------------------|------------------|------------------|
| Mean Ta ± SD / °C | 27.83 ± 0.40 | 3.37 ± 0.51 |
| Range / °C | 1.23 | 1.84 |
| Mean Rh ± SD / % | 49.25 ± 1.99 | 41.83 ± 2.66 |
| Range / % | 6.95 | 9.61 |

SD standard deviation

each sampling point. In winter, Ta gradually dopped from S07, remained low around S33 and gradually rose from S35, while Rh complies with an opposite trend. In summer, though data from S34 to S55 were removed due to anomaly, similar trend of Ta dropping while Rh rising at around S17 were observed from available data. The lowest two-day averaged Ta was recorded at S33 for summer (27.21 °C) and winter (2.30 °C), while the highest at S09 and S07 for summer (28.44 °C) and winter (4.14 °C) respectively. The lowest two-day averaged Rh was recorded at S07 for summer (48.84%) and winter (38.05%), while the highest at S62 and S36 for summer (52.79%) and winter (47.66%) respectively.

UGBS's local-scale climatic effects

Scale dependence of the relationship between Ta, Rh and land-cover and land-use factors

Figure 4 shows the Pearson correlation coefficient trends between Ta, Rh and land-cover and land-use factors represented by the percentage of 3 land-cover types and 14 LCZs within 100–1000m radius buffer zones.

All 3 land-cover types, i.e., vegetation, water and impervious surfaces, are significantly correlated with nighttime Ta and Rh in summer and winter, with stronger correlations detected for larger buffer zones. Vegetation and water coverage were significantly negatively correlated with Ta, while positively correlated with Rh, indicating a cooling and humidifying effect on summer and winter nights. While the impervious surface has an opposite effect. For land-use factors represented by coverage of different LCZs, correlations were not always detected among all LCZ types, and differences exist between two seasons. LCZ 1 and LCZ 2 are always positively correlated with Ta and negatively correlated with Rh in summer and winter, while LCZ 8, LCZ A and LCZ G comply with the opposite pattern. LCZ 3, negatively correlated with Ta and positively correlated with Rh in summer, is negatively correlated with Rh in winter. While LCZ 4 and LCZ 5, insignificant correlation with Ta in summer, are negatively correlated with Ta and positively correlated with Rh in winter. Similarly, stronger correlations are detected for larger buffer zones.

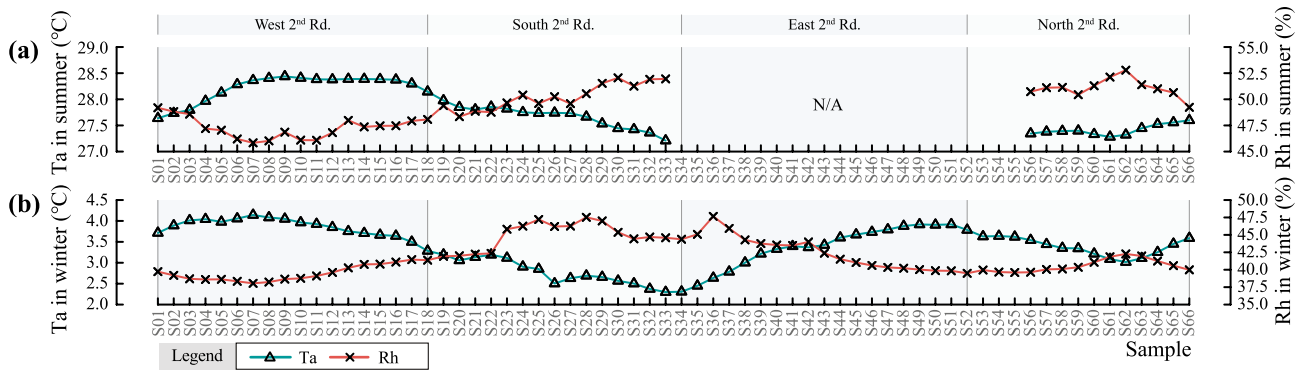


Fig. 3 Two-day averaged Ta and Rh profile along sampling routes in **a** summer and **b** winter

Urban vegetation and water coverage’s contribution to local scale climate

Figure 5 shows the linear regression models between centered Ta, Rh and percentage of different land-cover types within 1000m buffer zone. Better regression models are built for winter night with higher R² than summer night, indicating a more stable thermal environment at night in winter than in summer. Better regression models with higher R² were also built when considering urban vegetation and water coverage as a whole than taking urban vegetation solely into consideration.

By comparing the slopes of the regression models, increasing water coverage is more effective in cooling and humidifying than increasing vegetation coverage ($|\beta_V|=2.781 < |\beta_W|=10.179$, $|\beta_V|=17.390 < |\beta_W|=59.184$, $|\beta_V|=6.003 < |\beta_W|=17.584$, $|\beta_V|=28.830 < |\beta_W|=78.737$), though this is largely due to the rarity of water coverage in the study area. Stronger cooling and humidifying effects of urban vegetation and water coverage are also detected on winter night than summer. For every 10% increase in vegetation and water coverage, Ta may drop by 0.310 °C and 0.635 °C while Rh may increase by 1.896% and 2.988% on summer and winter nights respectively.

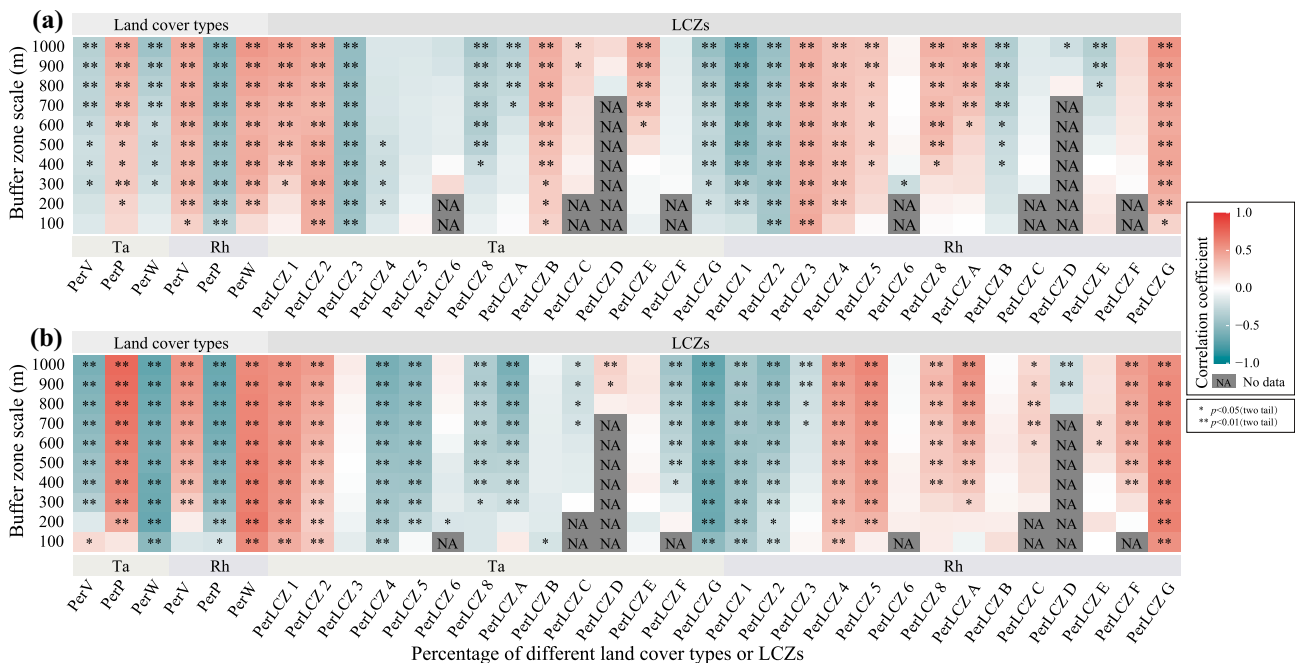


Fig. 4 Pearson correlation coefficients between Ta, Rh and the percentage of different land-cover types and LCZs within 100-1000m radius buffer zones in **a** summer and **b** winter. **PerV** Percentage of

vegetation coverage, **PerI** Percentage of impervious surfaces, **PerW** Percentage of water coverage, **PerLCZ x** Percentage of LCZ x

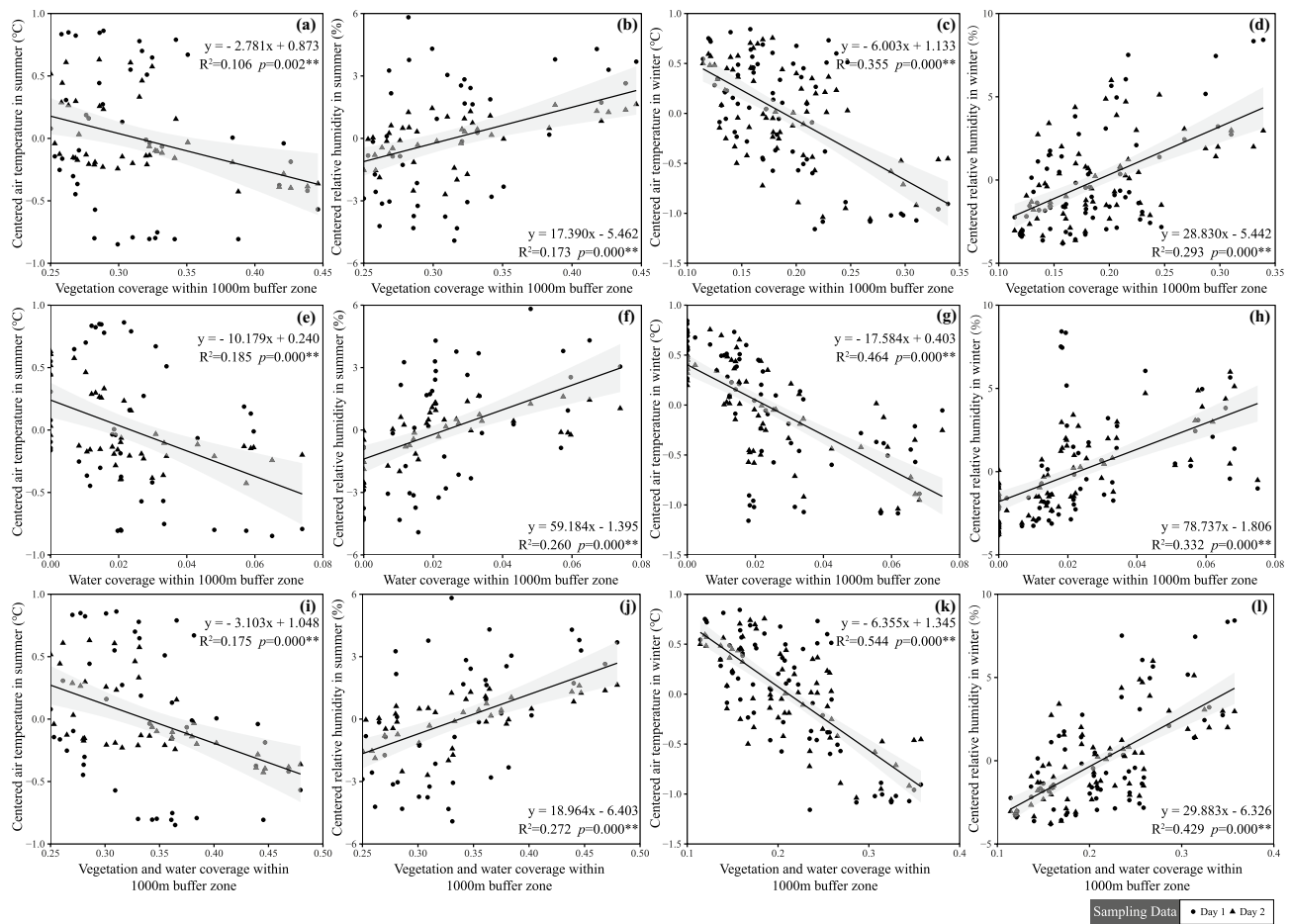


Fig. 5 Regression models with centered Ta and Rh as dependent variables and percentage of different land-cover types within 1000m buffer zone as independent variables (with shaded area representing 95% confidence interval)

Different LCZs’ contribution to local scale climate

Considering the definition of different LCZs that LCZ 1-6 are zones closely related to the building environment of residential and commercial uses, and the fact that LCZ 1-2 prevail but LCZ 3-6 are not so prevalent around the sampling routes, linear regression models were simply built between centered Ta, Rh and percentage of LCZ 1 and LCZ 2 within 1000m buffer zone, as shown in Fig. 5. By comparing the slopes of the regression models, compared with LCZ 2, LCZ 1 demonstrates a stronger effect of increasing Ta on summer and winter nights ($|\beta_1|=2.227 > |\beta_2|=1.255$, $|\beta_1|=2.476 > |\beta_2|=1.892$). And such Ta increasing and Rh decreasing effect of LCZ 1 and LCZ 2 are always stronger on winter nights than on summer.

We further constructed multiple regression models between centered Ta, Rh and different LCZ coverage within 1000m buffer zone, as shown in Table 2. Better regression models are built for Ta and Rh on winter nights than on summer, as indicated by higher R^2 ($R^2_w=0.707 > R^2_s=0.440$,

$R^2_w=0.615 > R^2_s=0.521$). LCZ 2 and LCZ G are 2 types of LCZs that universally included in all multiple regression models. By comparing the B coefficients in each model, coverage of LCZ G is found as the component contributing the most. On summer night, LCZ 1 outweighs LCZ 2 in decreasing Rh on summer night ($|B_1|=8.662 > |B_2|=2.539$). On winter night, LCZ 2 outweighs LCZ 1 in increasing Ta ($|B_1|=0.905 < |B_2|=1.216$), while LCZ 5 contributes to decreasing Ta ($B_5=-1.278$) and increasing Rh ($B_5=13.65$).

Urban vegetation’s contribution to local scale climate in different LCZs

To evaluate if the climatic effects of urban vegetation in different LCZs vary, correlation coefficients and partial correlation coefficients with total vegetation coverage controlled were calculated between centered Ta, Rh and vegetation coverage in LCZ 1-6 within 1000m buffer zone, as shown in Table 3. Results indicate that the climatic effects of vegetation in different types of LCZs vary. By controlling

Table 2 Multiple regression models between centered Ta, Rh in summer and winter and LCZ coverage within 1000m buffer zone

| | Summer nighttime Ta | | Summer nighttime Rh | | Winter nighttime Ta | | Winter nighttime Rh | |
|-------------------------|-------------------------|---------|---------------------|---------|-------------------------|---------|-------------------------|---------|
| | B | p | B | p | B | p | B | p |
| LCZ 1 | - | - | -8.662 | 0.000** | 9.052×10 ⁻¹ | 0.007** | - | - |
| LCZ 2 | 6.604×10 ⁻¹ | 0.013* | -2.539 | 0.038* | 1.216 | 0.000** | -5.068 | 0.000** |
| LCZ 5 | - | - | - | - | -1.278 | 0.008** | 1.365×10 | 0.000** |
| LCZ E | 5.655 | 0.000** | -1.944×10 | 0.001** | - | - | - | - |
| LCZ G | -8.593 | 0.000** | 2.723×10 | 0.009** | -1.203×10 | 0.000** | 5.913×10 | 0.000** |
| Intercept | -8.336×10 ⁻¹ | 0.000** | 4.098 | 0.000** | -1.907×10 ⁻¹ | 0.230 | -4.533×10 ⁻¹ | 0.400 |
| R ² | 0.440 | | 0.543 | | 0.707 | | 0.624 | |
| Adjusted R ² | 0.420 | | 0.521 | | 0.698 | | 0.615 | |
| p | 0.000** | | 0.000** | | 0.000** | | 0.000** | |

*p<0.05, **p<0.01, two tail. **B** Coefficient

total vegetation coverage, generally weaker correlation was found between Ta, Rh and vegetation coverage in different LCZs. While vegetation coverage in LCZ 2 still significantly contributed to decreasing Ta and increasing Rh on winter night (Par ρ=-0.29, 0.18). Vegetation in LCZ 3 was also found negatively correlated with Ta on summer night when controlling total vegetation coverage (Par ρ=-0.24).

Discussion

Urban climate is affected by multiple factors of urban form and geometry (Oke et al. 2017). In this study, we measured nighttime Ta and Rh along an enclosed route located at the city center of highly urbanized area in Beijing, China. Considering that the environment of the sampling route is universally open and unshaded, the main influencing factors on the measured climatic parameters are mainly variations in land-cover and land-use, which reflected both the urban fabric composition and the intensity of human activity.

We first evaluated to what distance does land-cover and land-use composition are correlated with field-measured Ta and Rh, and found that the correlations generally get stronger as the buffer zones get larger (Fig. 4), an issue also addressed by previous local studies (Fan et al. 2022; Qian et al. 2018;

Yan et al. 2014). Finding key thresholds in correlation coefficients is often the main concern of such studies. Though the measurement in this study was conducted on impervious surfaces as Yan et al. (2014) and Fan et al. (2022) did, threshold was not detected as they did. One main reason may lie in the difference in sampling environment, namely the width of the sampling route, 2nd Ring Rd., is much larger, resulting in that the near adjacent of each sampling point in our study is mainly impervious surfaces. This also gives explanation to insignificant relations for smaller buffer zones of 100-200m radius (Fig. 4). Similarly, in Qian et al. (2018)’s study, though their measurements were conducted solely in green spaces, homogenous green spaces in near adjacent also brought them difficulty in analyzing the spatial effect of green spaces. The heterogeneity of land-cover and land-use couldn’t be incorporated until buffer zones gradually get larger, which is different from measurements done in compact neighborhoods.

A three-class land-cover classification is applied in this study to analyze the contribution of different land-cover types on local climate at night, when atmospheric UHI effect, as well as the climatic effect of urban greenery, is stronger than daytime (Doick et al. 2014; Gao et al. 2019), which reaffirmed the cooling and humidifying effects of urban vegetation and water bodies (Bowler et al. 2010;

Table 3 Correlation coefficients and partial correlation coefficients with vegetation coverage controlled between centered Ta, Rh and vegetation coverage in LCZs 1-6 within 1000m buffer zone

| | LCZ 1 | | LCZ 2 | | LCZ 3 | | LCZ 4 | | LCZ 5 | | LCZ 6 | |
|--------------|---------------|-------|----------------|----------------|----------------|---------------|----------------|-------|----------------|----------------|----------------|----------------|
| | ρ | Par ρ | ρ | Par ρ | ρ | Par ρ | ρ | Par ρ | ρ | Par ρ | ρ | Par ρ |
| Ta in summer | 0.00 | -0.13 | 0.03 | 0.10 | -0.31** | -0.24* | -0.04 | -0.12 | 0.36** | 0.31* | 0.70** | 0.69** |
| Ta in winter | 0.07 | -0.01 | -0.47** | -0.29** | -0.22* | -0.03 | 0.20 | -0.05 | 0.20 | 0.21 | 0.04 | 0.53** |
| Rh in summer | -0.02 | 0.14 | -0.08 | -0.18 | 0.32** | 0.22 | -0.06 | 0.02 | -0.46** | -0.44** | -0.71** | -0.72** |
| Rh in winter | -0.20* | -0.16 | 0.38** | 0.18* | 0.26** | 0.10 | -0.35** | -0.19 | -0.26* | -0.27* | 0.01 | -0.39** |

*p<0.05, **p<0.01, two tail. ρ Correlation coefficients, **Par ρ** Partial correlation coefficients

Gunawardena et al. 2017; Wong et al. 2021). The mechanism of vegetation's nighttime cooling effect is complicated. At night, on one hand, tree canopy may hamper heat loss through influencing sky view factor and give rise to temperature (Taha 1997), while on the other hand, evapotranspiration effect of vegetation, though much weaker than daytime, still provides cooling (Snyder et al. 2003). Potent nighttime cooling and humidifying effects of green spaces in temperate regions have been recorded in previous empirical studies (Doick et al. 2014; Li et al. 2021a, b; Yan et al. 2018). Additionally, in winter, though the majority of trees in temperate regions are deciduous, evergreen trees demonstrate significant humidifying effects (Afshar et al. 2018; Li et al. 2020). Such evidences are in line with results in this study (Fig. 5a-d). Though water body serves as heat source due to its large heat capacity (Hathway and Sharples 2012; Steeneveld et al. 2014), results of this study indicate that vegetation and water bodies are both contributing to cooling and humidifying, and may best explain Ta and Rh variations when considered as a whole (Fig. 5i-l). One explanation is that water coverage is a rarity in the case of Beijing, and water bodies are usually closely combined with surrounding urban vegetation and their climatic effect are largely intertwined. It is therefore solid to count on construction of UGBS to overcome projected nighttime Ta rising in near future (Huang et al. 2021)s.

The measured Ta and Rh were also analyzed from the perspective of land-use by using adjacent LCZ composition. The thermal property difference among different LCZs is a synthesis of urban 3D morphology, land-cover condition, and human activity characteristics (Stewart and Oke 2012). One example on 3D morphology difference demonstrated in this study is the slopes of the models built between Ta, Rh and percentage of LCZ 1 (compact high-rise) and LCZ 2 (compact midrise) (Fig. 6), which reflects stronger heat production in LCZ 1 at night in summer and winter. Such results are in line with previous studies analyzing the interaction between 3D morphology and urban thermal environment (Chen et al.

2022; Tian et al. 2019; Zhou et al. 2022). Adjacent LCZ composition also well explained Ta and Rh variance in multiple regression models (Table 2). Similar to the models in Fig. 5, where enhancing water coverage was found more potent than vegetation in regulating local scale climate, LCZ G (water coverage), featuring largest coefficients, also outweighed other land-use in cooling and humidifying.

One aspect that LCZ scheme doesn't address is the precise depiction of urban vegetation, but just general depiction of greenery coverage difference by distinguishing compact land-use (LCZ 1-3) and open land-use (LCZ 4-6). The climatic effect of such vegetation coverage difference is reflected in multiple regression models (Table 2), where compact land-use (LCZ 1 and 2) were found increasing Ta and decreasing Rh while open land-use (LCZ 5) was found the opposite effect. Considering that the measurement was taken on impervious surfaces, i.e. LCZ E, it can be inferred that the higher vegetated area coverage in LCZ 5 is contributing to regulating local climate.

Enhancing green space ratio has long been proved as an effective way to cool the city (Bowler et al. 2010; Derdouri et al. 2021), which is also reassured in this study (Fig. 5). Additionally, previous studies tend to believe that the effect of land-cover composition outweighs that of urban green spaces' configuration (Guo et al. 2020; Masoudi et al. 2019; Naeem et al. 2018). However, considering that infinitely increasing green spaces coverage in urban areas is unrealistic, further knowledge is still needed on where and how to allocate green spaces for more effective regulating effect. In this study, results of partial correlation analysis may serve as a way to answer this question, for it indicates that enhancing vegetation coverage in LCZ 2 and 3 is linked with better cooling (Table 3). Considering that LCZ 2 was found facing more severe heat stress (Benjamin et al. 2021; Chen et al. 2021), future construction of urban green spaces in LCZ 2 and 3 is expected to contribute to not only microclimate within these land-use (Fan et al. 2017), but also nearby local-scale climate.

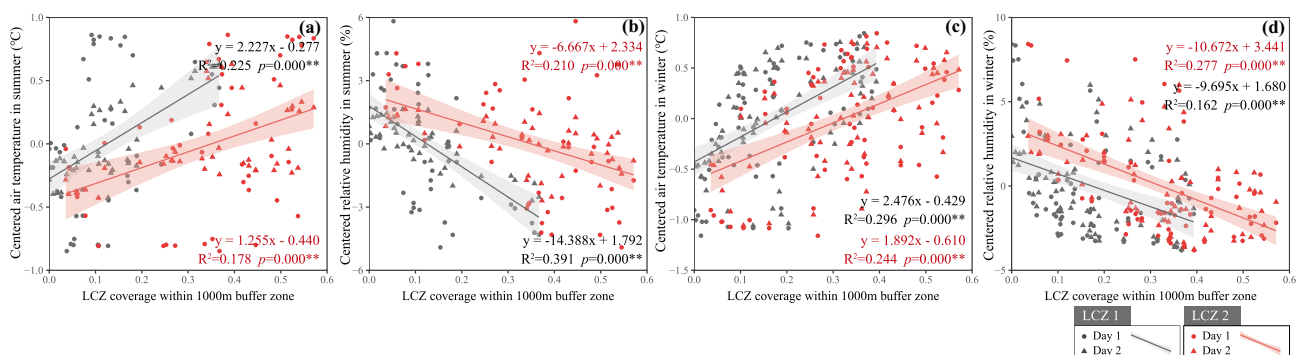


Fig. 6 Regression models with centered Ta and Rh as dependent variables and percentage of LCZ 1 and LCZ 2 within 1000m buffer zone as independent variables (with shaded area representing 95% confidence interval)

While significant correlations were also detected between vegetation coverage in LCZ 5 and 6 with climatic parameters which seems unreasonable (Table 3). Considering that these samples with LCZ 5 coverage are mostly located along South 2nd Rd. (S21-S38), where several large urban parks were nearby and therefore features high vegetation coverage (Figs. 1 and 2), vegetation coverage in built LCZs may not contribute as significantly as surrounding large parks to local scale climate (Li et al. 2021a, b), therefore resulting in such unexplainable results.

One limitation of this study is that it didn't distinguish the socio-economic characteristic of different land-use, which is also pointed out as one aspect that LCZ scheme doesn't well reflect (Yu et al. 2021). Though the difference of human metabolism among different LCZs is considered (Stewart and Oke 2012), detailed depiction of human activity and anthropogenic heat pattern are not reflected, which contributes to the daily and seasonal variation of urban climate (Aslam and Rana 2022; Sun et al. 2013). In this study, though not quantitatively analyzed, high Ta and low Rh were recorded on west (S05-S17) and north-east (S40-S59) 2nd Ring Rd. (Fig. 3), which is mainly surrounded by commercial and residential lands, the ones identified as main anthropogenic heat source (Hu et al. 2022; Sun et al. 2018). Incorporating socio-economic perspective to further investigation on the climatic effect difference of urban green and blue spaces in different land-use is still needed.

Conclusion

In this study, field measurements of nighttime Ta and Rh were conducted along an enclosed transect at the core area of Beijing, China. Three land-cover types, i.e., impervious surfaces, vegetation and water coverage, and LCZ scheme were used to analyze measured Ta and Rh. Urban vegetation coverage is further interested with LCZs to evaluate vegetation's cooling and humidifying effects in different land-uses. Ta and Rh variance were depicted along the transect at night in summer and winter. Better correlations were generally detected with larger buffer zones when more land-use and land-cover conditions were included. Urban green and blue spaces exhibit significant cooling and humidifying effects, and better regression models were built when green and blue spaces were taken as a whole rather than independently. Coverage of LCZ 1 (compact high-rise), LCZ 2 (compact midrise) and LCZ G (water coverage) significantly contribute to local-scale climate. Increasing vegetation coverage in LCZ 2 and LCZ 3 is expected to facilitate better local-scale cooling and humidifying effect. Further evaluation of urban vegetation's cooling and humidifying efficiency of in different land-uses is still needed to provide guidance for future urban green spaces planning and design.

Supplementary Information The online version contains supplementary material available at <https://doi.org/10.1007/s11252-023-01405-0>.

Acknowledgement We acknowledge Mr. Jin Li's assistance on data sampling. We also thank the editors and anonymous reviewers for processing and improving the quality of this manuscript.

Authors' contributions Yilun Li: Conceptualization, Methodology, Formal analysis, Investigation, Writing-Original Draft, Writing-Reviewing and Editing; Shuxin Fan: Methodology, Writing-Original Draft, Writing-Reviewing and Editing; Kun Li: Writing-Reviewing and Editing; Kaien Ke: Investigation; Li Dong: Resources, Supervision, Project administration, Funding acquisition, Writing-Reviewing and Editing.

Funding This study is funded by Beijing Municipal Science and Technology Commission (D171100007117001, D171100007117003).

Availability of data and material Data and material can be shared under reasonable request delivered to the corresponding author.

Code availability Code for data analysis can be shared under reasonable request delivered to the corresponding author.

Declarations

Ethics approval Not applicable.

Consent to participate Not applicable.

Consent for publication Not applicable.

Conflicts of interest Authors declare no competing interests as defined by Springer, or other interests that might be perceived to influence the results and/or discussion reported in this paper.

References

- Afshar NK, Karimian Z, Doostan R, Nokhandan MH (2018) Influence of Planting Designs on Winter Thermal Comfort in an Urban Park. *J Environ Eng Landsc* 26(3):232–240. <https://doi.org/10.3846/jeelm.2018.5374>
- Alexander PJ, Fealy R, Mills GM (2016) Simulating the impact of urban development pathways on the local climate: A scenario-based analysis in the greater Dublin region, Ireland. *Landsc Urban Plan* 152:72–89. <https://doi.org/10.1016/j.landurbplan.2016.02.006>
- Amani-Beni M, Chen Y, Vasileva M, Zhang B (2022) Quantitative-spatial relationships between air and surface temperature, a proxy for microclimate studies in fine-scale intra-urban areas. *Sustain Cities Soc* 77. <https://doi.org/10.1016/j.scs.2021.103584>
- Aslam A, Rana IA (2022) The use of local climate zones in the urban environment: A systematic review of data sources, methods, and themes. *Urban Clim* 42. <https://doi.org/10.1016/j.uclim.2022.101120>
- Benjamin K, Luo Z, Wang X (2021) Crowdsourcing urban air temperature data for estimating urban heat island and building heating/cooling load in London. *Energies* 14(16). <https://doi.org/10.3390/en14165208>
- Bowler DE, Buyung-Ali L, Knight TM, Pullin AS (2010) Urban greening to cool towns and cities: A systematic review of the empirical evidence. *Landscape and Urban Planning* 97(3):147–155. <https://doi.org/10.1016/j.landurbplan.2010.05.006>

- Chen J, Zhan W, Du P, Li L, Li J, Liu Z, Huang F, Lai J, Xia J (2022) Seasonally disparate responses of surface thermal environment to 2D/3D urban morphology. *Build Environ* 214. <https://doi.org/10.1016/j.buildenv.2022.108928>
- Chen X, Yang J, Ren C, Jeong S, Shi Y (2021) Standardizing thermal contrast among local climate zones at a continental scale: Implications for cool neighborhoods. *Build Environ* 197. <https://doi.org/10.1016/j.buildenv.2021.107878>
- Chen Y-C, Lo T-W, Shih W-Y, Lin T-P (2019) Interpreting air temperature generated from urban climatic map by urban morphology in Taipei. *Theoretical and Applied Climatology* 137(3–4):2657–2662. <https://doi.org/10.1007/s00704-018-02764-x>
- Connors JP, Galletti CS, Chow WTL (2012) Landscape configuration and urban heat island effects: assessing the relationship between landscape characteristics and land surface temperature in Phoenix, Arizona. *Landscape Ecology* 28(2):271–283. <https://doi.org/10.1007/s10980-012-9833-1>
- Dan Y, Li H, Jiang S, Yang Z, Peng J (2022) Changing coordination between urban area with high temperature and multiple landscapes in Wuhan City, China. *Sustain Cities Soc* 78. <https://doi.org/10.1016/j.scs.2021.103586>
- Demuzere M, Orru K, Heidrich O, Olazabal E, Geneletti D, Orru H, Bhawe AG, Mittal N, Feliu E, Faehnle M (2014) Mitigating and adapting to climate change: Multi-functional and multi-scale assessment of green urban infrastructure. *Journal of Environmental Management* 146:107–115. <https://doi.org/10.1016/j.jenvman.2014.07.025>
- Derdouri A, Wang R, Murayama Y, Osaragi T (2021) Understanding the Links between LULC Changes and SUHI in Cities: Insights from Two-Decadal Studies (2001–2020). *Remote Sens* 13(18). <https://doi.org/10.3390/rs13183654>
- Doick KJ, Peace A, Hutchings TR (2014) The role of one large greenspace in mitigating London's nocturnal urban heat island. *Sci Total Environ* 493:662–671. <https://doi.org/10.1016/j.scitotenv.2014.06.048>
- Dorigon LP, Amorim MCDCT (2019) Spatial modeling of an urban Brazilian heat island in a tropical continental climate. *Urban Clim* 28. <https://doi.org/10.1016/j.uclim.2019.100461>
- Eliasson I (2000) The use of climate knowledge in urban planning. *Landsc Urban Plan* 48(1–2):31–44. [https://doi.org/10.1016/S0169-2046\(00\)00034-7](https://doi.org/10.1016/S0169-2046(00)00034-7)
- Ellefsen R (1991) Mapping and measuring buildings in the canopy boundary layer in ten U.S. cities. *Energy Build* 16(3–4), 1025–1049. [https://doi.org/10.1016/0378-7788\(91\)90097-m](https://doi.org/10.1016/0378-7788(91)90097-m)
- Fan S, Li X, Han J, Hao P, Dong L (2017) Assessing the effects of landscape characteristics on the thermal environment of open spaces in residential areas of Beijing China. *Landsc Ecol Eng* 14(1):79–90. <https://doi.org/10.1007/s11355-017-0326-x>
- Fan S, Li Y, Zhang M, Li K, Xie Y, Dong L (2022) Spatial differentiation of neighborhood climates and their response to surrounding land cover composition: A case study in Beijing, China. *Sci Total Environ* 826, 154001. <https://doi.org/10.1016/j.scitotenv.2022.154001>
- Gago EJ, Roldan J, Pacheco-Torres R, Ordóñez J (2013) The city and urban heat islands: A review of strategies to mitigate adverse effects. *Renew Sustain Energy Rev* 25:749–758. <https://doi.org/10.1016/j.rser.2013.05.057>
- Gao Z, Hou Y, Chen W (2019) Enhanced sensitivity of the urban heat island effect to summer temperatures induced by urban expansion. *Environ Res Lett* 14(9). <https://doi.org/10.1088/1748-9326/ab2740>
- Grimmond SUE (2007) Urbanization and global environmental change: local effects of urban warming. *Geogr J* 173(1):83–88. https://doi.org/10.1111/j.1475-4959.2007.232_3.x
- Gunawardena KR, Wells MJ, Kershaw T (2017) Utilising green and bluespace to mitigate urban heat island intensity. *Sci Total Environ* 584–585:1040–1055. <https://doi.org/10.1016/j.scitotenv.2017.01.158>
- Guo G, Wu Z, Cao Z, Chen Y, Yang Z (2020) A multilevel statistical technique to identify the dominant landscape metrics of greenspace for determining land surface temperature. *Sustain Cities Soc* 61. <https://doi.org/10.1016/j.scs.2020.102263>
- Hathway EA, Sharples S (2012) The interaction of rivers and urban form in mitigating the Urban Heat Island effect: A UK case study. *Build Environ* 58:14–22. <https://doi.org/10.1016/j.buildenv.2012.06.013>
- Hu D, Meng Q, Schlink U, Hertel D, Liu W, Zhao M, Guo F (2022) How do urban morphological blocks shape spatial patterns of land surface temperature over different seasons? A multifactorial driving analysis of Beijing, China. *Int J Appl Earth Observ and Geoinfo* 106. <https://doi.org/10.1016/j.jag.2021.102648>
- Hu Y, Hou M, Jia G, Zhao C, Zhen X, Xu Y (2019) Comparison of surface and canopy urban heat islands within megacities of eastern China. *ISPRS Journal of Photogrammetry and Remote Sensing* 156:160–168. <https://doi.org/10.1016/j.isprsjprs.2019.08.012>
- Huang K, Lee X, Stone B, Kniviel J, Bell ML, Seto KC (2021) Persistent Increases in Nighttime Heat Stress From Urban Expansion Despite Heat Island Mitigation. *J Geophys Res Atmos* 126(4). <https://doi.org/10.1029/2020jd033831>
- International Standard Organization (1998) ISO 7726, Thermal environments: Instruments and Methods for Measuring Physical Quantities. ISO, Geneva
- Karasiak N (2016) DZetsaka Qgis Classification plugin
- Ke X, Men H, Zhou T, Li Z, Zhu F (2021) Variance of the impact of urban green space on the urban heat island effect among different urban functional zones: A case study in Wuhan. *Urban For Urban Green* 62. <https://doi.org/10.1016/j.ufug.2021.127159>
- Lecote F, Bouyer J, Claverie R, Pétrissans M (2015) Using Local Climate Zone scheme for UHI assessment: Evaluation of the method using mobile measurements. *Building and Environment* 83:39–49. <https://doi.org/10.1016/j.buildenv.2014.05.005>
- Li T, Xu Y, Yao L (2021a) Detecting urban landscape factors controlling seasonal land surface temperature: from the perspective of urban function zones. *Environ Sci Pollut Res Int* 28(30):41191–41206. <https://doi.org/10.1007/s11356-021-13695-y>
- Li Y, Fan S, Li K, Zhang Y, Dong L (2020) Microclimate in an urban park and its influencing factors: a case study of Tiantan Park in Beijing, China. *Urban Ecosystems* 24(4):767–778. <https://doi.org/10.1007/s11252-020-01073-4>
- Li Y, Fan S, Li K, Zhang Y, Kong L, Xie Y, Dong L (2021b) Large urban parks summertime cool and wet island intensity and its influencing factors in Beijing, China. *Urban For Urban Green* 65. <https://doi.org/10.1016/j.ufug.2021.127375>
- Masoudi M, Tan PY, Fadaei M (2021) The effects of land use on spatial pattern of urban green spaces and their cooling ability. *Urban Clim* 35. <https://doi.org/10.1016/j.uclim.2020.100743>
- Masoudi M, Tan PY, Liew SC (2019) Multi-city comparison of the relationships between spatial pattern and cooling effect of urban green spaces in four major Asian cities. *Ecol Indic* 98:200–213. <https://doi.org/10.1016/j.ecolind.2018.09.058>
- Naeem S, Cao C, Qazi W, Zamani M, Wei C, Acharya B, Rehman A (2018) Studying the Association between Green Space Characteristics and Land Surface Temperature for Sustainable Urban Environments: An Analysis of Beijing and Islamabad. *ISPRS Int J Geo-Info* 7(2). <https://doi.org/10.3390/ijgi7020038>
- National Bureau of Statistics of China (Beijing) (2020) Beijing Statistical Yearbook 2019 China Statistics Press, Beijing
- Nie T, Lai D, Liu K, Lian Z, Yuan Y, Sun L (2022) Discussion on inapplicability of Universal Thermal Climate Index (UTCI) for outdoor thermal comfort in cold region. *Urban Clim* 46. <https://doi.org/10.1016/j.uclim.2022.101304>
- Oke TR (1982) The energetic basis of the urban heat island. *Q J R Meteorol Soc* 108(455):1–24. <https://doi.org/10.1002/qj.49710845502>

- Oke TR (2005) Towards better scientific communication in urban climate. *Theor Appl Climatol* 84(1–3):179–190. <https://doi.org/10.1007/s00704-005-0153-0>
- Oke TR, Mills G, Christen A, Voogt JA (2017) *Urban Clim*. Cambridge University Press
- Peng J, Xie P, Liu Y, Ma J (2016) Urban thermal environment dynamics and associated landscape pattern factors: A case study in the Beijing metropolitan region. *Remote Sens Environ* 173:145–155. <https://doi.org/10.1016/j.rse.2015.11.027>
- Qian Y, Zhou W, Hu X, Fu F (2018) The Heterogeneity of Air Temperature in Urban Residential Neighborhoods and Its Relationship with the Surrounding Greenspace. *Remote Sens* 10(6). <https://doi.org/10.3390/rs10060965>
- Shi Y, Lau KK-L, Ren C, Ng E (2018) Evaluating the local climate zone classification in high-density heterogeneous urban environment using mobile measurement. *Urban Climate* 25:167–186. <https://doi.org/10.1016/j.uclim.2018.07.001>
- Shi Y, Xiang Y, Zhang Y (2019) Urban Design Factors Influencing Surface Urban Heat Island in the High-Density City of Guangzhou Based on the Local Climate Zone. *Sensors (Basel)* 19(16). <https://doi.org/10.3390/s19163459>
- Smith N, Georgiou M, King AC, Tiegies Z, Webb S, Chastin S (2021) Urban blue spaces and human health: A systematic review and meta-analysis of quantitative studies. *Cities* 119. <https://doi.org/10.1016/j.cities.2021.103413>
- Snyder KA, Richards JH, Donovan LA (2003) Night-time conductance in C3 and C4 species: do plants lose water at night? *J Exp Bot* 54(383):861–865. <https://doi.org/10.1093/jxb/erg082>
- Steeneveld GJ, Koopmans S, Heusinkveld BG, Theeuwes NE (2014) Refreshing the role of open water surfaces on mitigating the maximum urban heat island effect. *Landsc Urban Plan* 121:92–96. <https://doi.org/10.1016/j.landurbplan.2013.09.001>
- Stewart ID, Oke TR (2012) Local Climate Zones for Urban Temperature Studies. *Bull Am Meteorol Soc* 93(12):1879–1900. <https://doi.org/10.1175/bams-d-11-00019.1>
- Sun R, Lü Y, Chen L, Yang L, Chen A (2013) Assessing the stability of annual temperatures for different urban functional zones. *Build Environ* 65:90–98. <https://doi.org/10.1016/j.buildenv.2013.04.001>
- Sun R, Wang Y, Chen L (2018) A distributed model for quantifying temporal-spatial patterns of anthropogenic heat based on energy consumption. *J Clean Prod* 170:601–609. <https://doi.org/10.1016/j.jclepro.2017.09.153>
- Taha H (1997) Urban climates and heat islands: albedo, evapotranspiration, and anthropogenic heat. *Energy Build* 25(2):99–103. [https://doi.org/10.1016/s0378-7788\(96\)00999-1](https://doi.org/10.1016/s0378-7788(96)00999-1)
- Taylor L, Hochuli DF (2017) Defining greenspace: Multiple uses across multiple disciplines. *Landsc Urban Plan* 158:25–38. <https://doi.org/10.1016/j.landurbplan.2016.09.024>
- Tian Y, Zhou W, Qian Y, Zheng Z, Yan J (2019) The effect of urban 2D and 3D morphology on air temperature in residential neighborhoods. *Landsc Ecol* 34(5):1161–1178. <https://doi.org/10.1007/s10980-019-00834-7>
- Wang J, Zhou W, Jiao M (2022) Location matters: planting urban trees in the right places improves cooling. *Front Ecol Environ*. <https://doi.org/10.1002/fee.2455>
- Weber N, Haase D, Franck U (2014) Zooming into temperature conditions in the city of Leipzig: how do urban built and green structures influence earth surface temperatures in the city? *Sci Total Environ* 496:289–298. <https://doi.org/10.1016/j.scitotenv.2014.06.144>
- Wong NH, Tan CL, Kolokotsa DD, Takebayashi H (2021) Greenery as a mitigation and adaptation strategy to urban heat. *Nat Rev Earth Environ* 2(3):166–181. <https://doi.org/10.1038/s43017-020-00129-5>
- Yan H, Fan S, Guo C, Hu J, Dong L (2014) Quantifying the impact of land cover composition on intra-urban air temperature variations at a mid-latitude city. *PLoS One* 9(7), e102124. <https://doi.org/10.1371/journal.pone.0102124>
- Yan H, Wu F, Dong L (2018) Influence of a large urban park on the local urban thermal environment. *Sci Total Environ* 622–623:882–891. <https://doi.org/10.1016/j.scitotenv.2017.11.327>
- Yang X, Peng LLH, Chen Y, Yao L, Wang Q (2020) Air humidity characteristics of local climate zones: A three-year observational study in Nanjing. *Build Environ* 171. <https://doi.org/10.1016/j.buildenv.2020.106661>
- Yu Z, Jing Y, Yang G, Sun R (2021) A new urban functional zone-based climate zoning system for urban temperature study. *Remote Sens* 13(2). <https://doi.org/10.3390/rs13020251>
- Yu Z, Yang G, Zuo S, Jørgensen G, Koga M, Vejre H (2020) Critical review on the cooling effect of urban blue-green space: A threshold-size perspective. *Urban For Urban Green* 49. <https://doi.org/10.1016/j.ufug.2020.126630>
- Zhou L, Yuan B, Hu F, Wei C, Dang X, Sun D (2022) Understanding the effects of 2D/3D urban morphology on land surface temperature based on local climate zones. *Build Environ* 208. <https://doi.org/10.1016/j.buildenv.2021.108578>
- Zhou W, Huang G, Cadenasso ML (2011) Does spatial configuration matter? Understanding the effects of land cover pattern on land surface temperature in urban landscapes. *Landsc Urban Plan* 102(1):54–63. <https://doi.org/10.1016/j.landurbplan.2011.03.009>
- Zhou Y, Zhang G, Jiang L, Chen X, Xie T, Wei Y, Xu L, Pan Z, An P, Lun F (2021) Mapping local climate zones and their associated heat risk issues in Beijing: Based on open data. *Sustain Citi Soc* 74. <https://doi.org/10.1016/j.scs.2021.103174>

Springer Nature or its licensor (e.g. a society or other partner) holds exclusive rights to this article under a publishing agreement with the author(s) or other rightsholder(s); author self-archiving of the accepted manuscript version of this article is solely governed by the terms of such publishing agreement and applicable law.